Jurnal Ilmiah Teknik Elektro Komputer dan Informatika (JITEKI)
Vol. 10, No. 4, December 2024, pp. 833-842
ISSN: 2338-3070, DOI: 10.26555/jiteki.v10i4.30374

Comparative Analysis of Daily and Weekly Heavy Rain Prediction Using LSTM and Cloud Data

Vivi Monita, Sevirda Raniprima, Nanang Cahyadi
School of Electrical Engineering, Telkom University, Jakarta, Indonesia

ARTICLE INFO

Article history:

Received November 30, 2024
Revised December 19, 2024
Accepted December 31, 2024

Keywords:

Weather;
Heavy rain;
Deep learning;
LSTM

ABSTRACT

Indonesia's distinct geographic and climatic features make forecasting the weather there tricky. Due to its location at the equator and between two enormous oceans, the nation endures erratic weather patterns. Despite technical developments, the Meteorology, Climatology, and Geophysics Agency (BMKG) require assistance with precise forecasting. This research seeks to increase prediction accuracy using the Long Short-Term Memory (LSTM) algorithm, a deep learning technique appropriate for time series data processing. The research focuses on cloud data sets to improve the prediction of heavy rain. The potential of LSTM in weather forecasting has been demonstrated in earlier research, focusing on identifying rain at particular intervals. This research compares daily and weekly heavy rain prediction models using Python. Results reveal that the weekly model outperforms the daily model, achieving 85% accuracy compared to 80%. These findings highlight the effectiveness of LSTM in addressing the limitations of existing methods, offering a foundation for more reliable weather forecasting tailored to Indonesia's conditions.

Corresponding Author:

Vivi Monita, School of Electrical Engineering, Telkom University, Jakarta, Indonesia.
Email: mailto:monitavivii@telkomuniversity.ac.id

1. INTRODUCTION

In the modern era, meteorological information has become a basic need for various sectors of life, replacing its previous status as mere common knowledge. In Indonesia, weather prediction has become a fascinating subject, especially considering that the Meteorology, Climatology, and Geophysics Agency (BMKG) has repeatedly provided forecasts that are only sometimes wholly accurate [1]. It is essential to recognize that Indonesia, as an equatorial country, faces high uncertainty and rapid and complex weather changes [2]-[5]. In addition, the country's archipelagic landscape, located between two vast oceans, the Indian and Pacific, adds to the inherent complexity of predicting weather changes [6], [8].

In Indonesia, various observation techniques are used to forecast the weather, like a detective gathering evidence. These methods include weather stations, traditional radiosondes, airplane measurements, meteorological observations, and remote sensing devices like satellites and radar [7]. Satellites are crucial among these techniques because they act as "eyes in the sky" that continuously monitor atmospheric conditions. Himawari-8 is one of the most essential satellites [9]-[12]. Its ability to gather numerical data is necessary for creating more precise weather forecasts.

Numerous investigations have been carried out to identify and forecast rainfall in Indonesia. Data from the Himawari-8 satellite, the newest geostationary satellite created by JMA/JAXA (Japan Meteorological Agency/Japan Aerospace Exploration Agency), was specifically used in one of these studies. Since its launch on October 7, 2014, the Himawari-8 satellite has been delivering observation data since July 7, 2015 [5].

Numerous earlier studies on weather prediction have been carried out, including the use of the LSTM algorithm for weather prediction processing [13], [17], deep learning techniques for weather data analysis [14]-

[16], and numerical data processing using the Weather Research and Forecasting (WRF) model and multicasting techniques that are downscaled from the Global Forecast System (GFS) output [18].

Several earlier studies have focused on a few key approaches to developing weather prediction techniques: modeling using Brightness Temperature (BT) and Brightness Temperature Difference (BTD) data [19]-[20], deep learning techniques using Himawari-8 satellite data processing or related data [21]-[24], and the use of the LSTM algorithm [22].

Rainfall prediction modeling with Brightness Temperature (BT) and Brightness Temperature Difference (BTD) data shows that not all BTD scenarios are suitable for heavy rainfall prediction [23]-[26]. This highlights the need to select the appropriate BTD scenario to improve prediction accuracy. Himawari-8 data processing using the Rapid Developing Cumulus Area (RDCA) method shows effective potential in detecting and predicting heavy rainfall events in Indonesia with lighter rainfall being more accessible to predict than heavier rainfall [27]. A deep learning approach for heavy rainfall prediction using RDCA and Himawari-8 data shows that the more training iterations, the more performance improves [28]-[30]. In addition, another study using RN-NET with radar data for rainfall prediction has good accuracy scores using prediction time durations of 0.5 hours, 1 hour, and 2 hours [31]-[35]. Comparison of forecast results without and using the latest satellite imagery data with the ConvLSTM model shows that using satellite imagery data and cloud imagery, forecasts can help understand insolation, prevent incorrect predictions, and improve prediction accuracy [36]. However, ConvLSTM is best used for image or video data [37], [39]. Based on other literature studies, using LSTM nowcasting or LSTM forecasting for rain detection has fewer errors [38], [42]. In addition, rain prediction with LSTM on Himawari data is accurate [40]-[44]. These findings indicate that deep learning algorithms or LSTM have further opportunities to be developed by modeling rain prediction time for 1 hour or 2 hours.

Therefore, this research aims to address the challenges of heavy rain prediction in Indonesia by developing an accurate model using cloud data from the Himawari-8 satellite and the Long Short-Term Memory (LSTM) deep learning algorithm. The study focuses on comparing the performance of daily and weekly prediction models for heavy rain in West Jakarta City. Ten key parameters from the Himawari-8 satellite are analyzed to optimize prediction accuracy, focusing on bands 3, 8, 10, 11, and 13. These bands were selected based on their sensitivity to cloud properties and atmospheric conditions, which are critical for detecting heavy rain patterns. The methodology builds on prior studies by addressing limitations in satellite data processing and deep learning approaches, providing a robust framework for improving prediction accuracy tailored to Indonesia's unique climatic challenges.

2. RESEARCH METHODS

This stage explains the method used in this research, which consists of three stages: data conversion, creating a prediction model with LSTM, and simulating the LSTM model.

This research uses the Himawari-8 satellite dataset from February 1, 2023, to March 31, 2023. This dataset was downloaded from the JMA/JAXA (Japan Meteorological Agency/Japan Aerospace Exploration Agency) website using FileZilla version 3.63.2.1. The downloaded data is still in NetCDF format, so it is necessary to convert it to CSV to make it easier to process using Python version 3.9. The data conversion flow is shown in Fig. 1 (a).

The dataset conversion process in Fig. 1 (a) begins by downloading the NetCDF dataset from February 1, 2023, to March 31, 2023, via the JMA/JAXA website with FilleZila. Initialize the dataset date. This program converts data for 1 day with an average number of NetCDF datasets per day of around 124 data or every 10 minutes. Then the process continues by loading the NetCDF dataset using the Python program to view the data contents consisting of headers such as 'latitude,' 'longitude,' 'band_id,' 'start_time,' 'end_time,' 'geometry_parameters,' 'albedo_01', 'albedo_02', 'albedo_03', 'sd_albedo_03', 'albedo_04', 'albedo_05', 'albedo_06', 'tbb_07', 'tbb_08', 'tbb_09', 'tbb_10', 'tbb_11', 'tbb_12', 'tbb_13', 'tbb_14', 'tbb_15', 'tbb_16', 'SAZ,' 'SAA,' 'SOZ,' 'SOA,' and 'Hour.' The process continues by taking bands 3, 8, 10, 11, and 13 and deleting 20 initial data considered noise. Then, the initialization process of the longitude and latitude of West Jakarta City is entered. Fill in the band data based on the longitude and latitude of West Jakarta City. Change the 2D array from the NetCDF dataset to a 1D array. Calculate ten rain detection parameters with bands 3, 8, 10, 11, and 13. Save the calculation results in a new variable with a list form. The data content will be empty if the band or calculation result has no value. Then, add each new value in list format to the variable to be converted into CSV format. The index of the resulting CSV data set is the date of each data set. The model creation process in Fig. 1 (b) starts with initializing the file location, name, and several additional variables; after initialization, the data file is loaded according to its name. Error checking is done for further data processing; if there is no error, then the header data is printed, and then the data. Finding all columns with empty data, check again to ensure no missing value files are left. To fill in missing values, first check for linearity in each column using an autocorrelation plot.

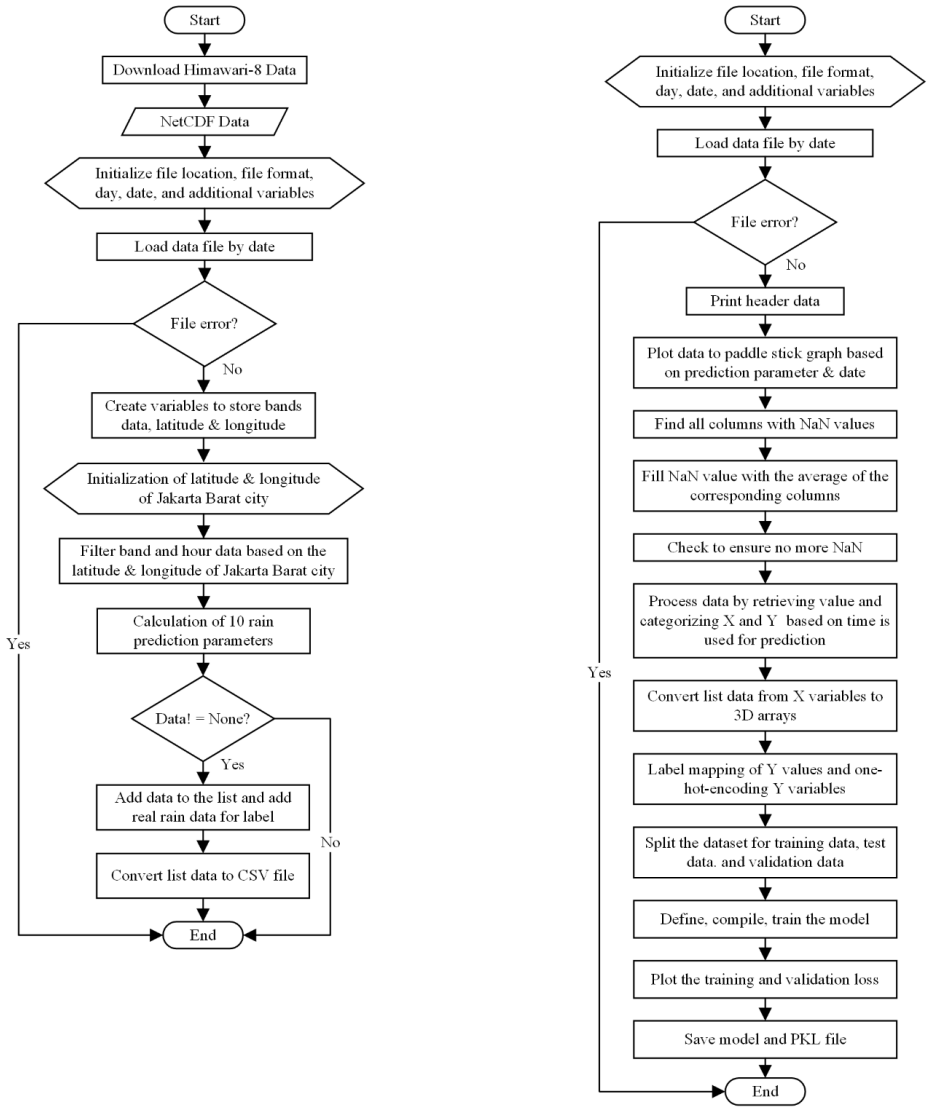

(a) (b)

Fig. 1. Flowchart (a) Data conversion (b) Prediction model

Then, fill in the missing values with the average of the corresponding columns. If the filling is successful, it will appear. After the data is cleaned and confirmed free of anomalies, the next step is to determine the features for the predictor parameters (X) and target parameters (Y). Determination of these features is done by considering the relationship between the parameters relevant to the prediction of heavy rain. Furthermore, the X and Y data are grouped based on daily and weekly prediction needs. The data will be grouped into six rows (daily model) or 12 rows (weekly model) of CSV data with the probability label calculated as heavy rain. If the probability of rain is more than 0.5, it is considered heavy rain. This is done to evaluate the temporal order and past influence on the prediction.

After the dataset grouping is complete, enter the separation of the X and Y value parameters and then group them based on the time used for prediction (daily or weekly), after which the list of data results is converted from the X variable to a 3D array. The Y variable is made by label mapping. One-Hot-Encoding Variable: After the X and Y feature data are ready, the next step is to map the labels for the target parameter (Y). The data in the Y parameter, initially a string, is converted into a numeric representation using the one-hot encoding technique. This technique transforms the "Heavy Rain" label into a "1" vector and the "No Rain" label into a "0" vector. For the daily and weekly model labels, the data set uses the probability labels that have been grouped. If the score is above 0.5, it is included in the Heavy Rain condition and vice versa. This is done to speed up data processing with machine learning algorithms. Separate the training and testing data set as shown in Table 1.

After obtaining the model, it enters the simulation process using new data. The prediction simulation begins by initializing the file location, name, and variables. Load the previously modeled PKL file, check for errors from the file, and then load the data from the file. The following process takes the value of the parameter variable X and converts the X data list into a 3D array. The last process is to predict data based on each existing model so that each processed data will produce prediction results [15]. The process flow is shown in Fig. 2.

Table 1. Training shape dimension dataset for daily and weekly models

Shape Datasets	Daily Model	Weekly Model
x_train	6986, 6, 13	6981, 12, 13
y_train	6986, 2	6981, 2
x_test	1747, 6, 13	1746, 12, 13
y_test	1747, 2	1746, 2

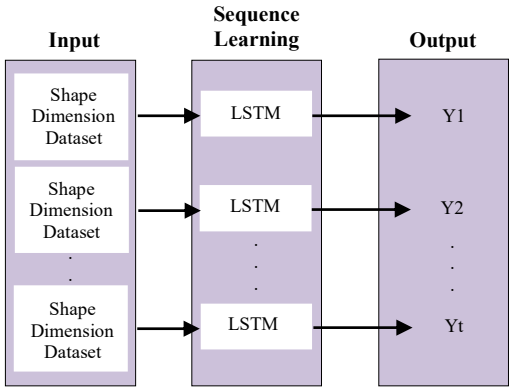

Fig. 2. LSTM simulation process

2.1. Himawari-8 Satellite

The Space Environment Data Acquisition Monitor (SEDA) aboard the Himawari-8 satellite monitors high-energy protons and electrons in orbit. The Environmental Monitoring Unit (EMU) created for the Galileo satellite is the foundation for SEDA, which RUAG Space provides. The Advanced Himawari Imager (AHI), an optical sensor on the Himawari-8 satellite, operates in the thermal and reflecting spectrum. For optimal coverage of East Asia to the western Pacific, data is recorded every 10 minutes; for specific observations, data is recorded every 2.5 minutes. Ten infrared (IR) channels, three visible channels, and three near-infrared (NIR) channels make up the 16 channels of the Himawari-8 satellite [16], [17]. There are multiple formats for Himawari-8 picture data, including Network Common Data Format (NetCDF), Portable Network Graphics (PNG), Low-Rate Information Transmission (LRIT), Himawari Standard Format (HSF), and HRIT. NMHS receives all satellite images via the Himawari Cloud service. Multidimensional data sets are stored, manipulated, and accessed using CDF, a conceptual data abstraction employed in this study with NetCDF. This CDF format is readable and writeable in several programming languages, including Python, C, FORTRAN, Java, MATLAB, and others. Time, latitude, and longitude are the three dimensions of CDF [18]. This research uses bands 3, 8, 10, 11, and 13 because it focuses on cloud data available on Himawari-8 satellite data. The selection of bands 3, 8, 10, 11, and 13 in Himawari-8 satellite data was made because of their relevant characteristics for cloud analysis. Band 3 (0.64 µm) is used to detect cloud details such as pattern, structure, and coverage with high resolution. Band 8 (6.2 µm) measures the radiation of air vapor in the upper atmosphere to study the distribution of air vapor and the location of high clouds. Band 10 (7.3 µm) focuses on the middle atmosphere, separating high and low clouds and determining cloud top temperatures. Band 11 (8.6 µm) detects the physical characteristics of clouds, such as particle composition (air or ice). In comparison, Band 13 (10.4 µm) is ideal for observing cloud top temperatures, helping to identify cold clouds associated with storms and significant weather systems.

2.2. Long-Short Term Memory (LSTM)

LSTM is a type of artificial neural network that belongs to the RNN (Recurrent Neural Network) class and is designed to overcome the problem of learning long-term dependencies in sequential data. Unlike ordinary RNNs that experience vanishing gradient problems, LSTM can retain essential information over a more extended period. Each neuron in LSTM functions as a memory unit equipped with three types of gates: input gate (IG), forget gate (FG), and output gate (OG). The input gate determines what new information will

be stored, the forget gate decides which data needs to be deleted, and the output gate regulates the information forwarded to the next step. With this mechanism, LSTM can adaptively manage relevant information, making it suitable for various applications such as natural language processing, time series data prediction, and pattern recognition [19].

$$f_t = \sigma(U_t h_{t-1} + W_f x_t) \quad (1)$$

$$k_t = c_{t-1} f_t \quad (2)$$

$$i_t = \sigma(U_i h_{t-1} + W_i x_t) \quad (3)$$

$$g_t = tanh(U_g h_{t-1} + W_g x_t) \quad (4)$$

$$j_t = g_t i_t \quad (5)$$

$$c_t = j_t + k_t \quad (6)$$

$$o_t = \sigma(U_o h_{t-1} + W_o x_t) \quad (7)$$

$$h_t = tanh(c_t) o_t \quad (8)$$

To determine whether information should be forgotten (deleted), the LSTM unit contains an FG. After reading $h_{(t-1)}$ and x_t, this gate outputs f_t between 0 and 1. The LSTM unit's current state, $c_{(t-1)}$, will be updated by this ft value. To put it briefly, the FG will either successfully save or forget the data from the IG and the prior LSTM unit. After that, the FG feeds the behavioral recognition system the frame image sequence that already exists. Equation (2) and Equation (3) formulate the LSTM structure [20].

IG will provide the cloud feature information that x_t. The output data from the preceding LSTM cell is shown in $h_{(t-1)}$; the sigmoid layer is represented by σ. FG provides U_t with the input coefficient matrix information; The cell state from the preceding LSTM cell is represented by $c_{(t-1)}$, W_f represents the network coefficient matrix from FG, and the FG output utilized to update the current cell condition is represented by k_t [20].

The IG processes the input data to the current unit after the LSTM unit forgets the current state information. It is crucial to combine $h_{(t-1)}$ and x_t with a sigmoid layer to identify the data that needs to be updated in the current unit. After that, $h_{(t-1)}$ and x_t can be processed with the aid of the tanh activation function to provide fresh candidate unit information as extra data. Equations (4) through (7) provide the process formula [20].

The sigmoid layer (σ) in the LSTM unit's OG gathers information about output condition evaluation. The tanh layer then obtains the vector between decisions at [-1, 1]. For the LSTM unit result, the resultant vector is then multiplied by the IG result. OG will normalize the final data for heavy rain prediction during the procedure. Equations (8) provide a mathematical explanation for this section [20].

3. RESULTS AND DISCUSSION

3.1. Results

This section will discuss the simulations' results and training analysis on heavy rain prediction models with daily and weekly prediction models.

The dataset used in this research is obtained through a conversion process that involves calculating ten rain detection parameters, ensuring comprehensive analysis and accurate detection. For bands 3, 8, 10, 11, and 13, the calculation process specifically employs statistical measures, including standard deviation, reduction, and average, as defined by Equations (7) to (8). These calculations help extract meaningful features from the data, enabling the identification of rain-related patterns. The outcome of this conversion process, which translates raw satellite data into structured information for analysis, is visually represented in Fig. 3, providing a clear depiction of the dataset's transformed state.

In Fig. 3, the values of the ten rain detection parameters have different data distributions. However, some are the same, such as (1) Parameters 1, 4, and 10; (2) Parameter 7; (3) Parameters 8 and 9; and (4) Parameters 3, 5, 6, and 13. If you look at the relationship with the data label it is shown in Fig. 3.

In the label graph, Fig. 4 shows only 1 and 0, with label 1 representing a heavy rain condition and label 0 representing a no rain condition. The heavy rain condition in Fig. 4 starts at 12.10 and goes up to 1.40 WIB, with different feature conditions for each parameter.

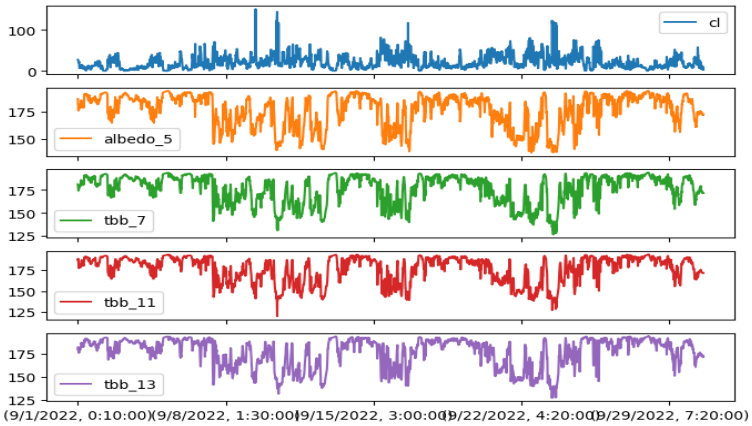

Fig. 3. Training and validation graphs for loss and accuracy of 100 daily model iterations

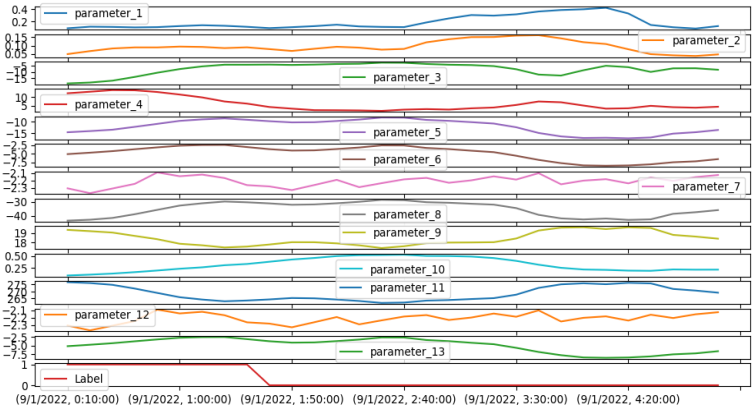

Fig. 4. Relationship between ten parameters and heavy rainfall conditions

The model training experiment on the Himawari-8 satellite dataset was conducted to obtain a heavy rainfall prediction model with good accuracy for each parameter combination. The parameter combination is based on the data distribution and is divided into two categories: no rain and heavy rain. This experiment uses two timing models, namely daily modeling and weekly modeling. The training data and test data are divided into a composition of 80% and 20% with the LSTM architecture limited to experiments with 50 hidden layers and 100 hidden layers. Based on the results of the model training that has been obtained, the model with the best accuracy and RMSE and MAE values approaching 0 is the weekly F4 with 100 hidden layers. Followed by the weekly F4 model with 50 hidden layers, daily F4 with 100 hidden layers, and all weekly with 100 hidden layers. The four models have an accuracy above 81%, with accuracies of 95%, 87%, 85%, and 82%, respectively.

To provide strong validation, testing was continued using new data calculated from May 1, 2023, to May 5, 2023, with a total of 669 rows of data. The results of the accuracy validation with new data from the four models are shown in Table 2.

Table 2. Model training summary

Hidden Layer	Pattern	Test Accuracy (%)	No Rain (%)	Heavy Rain (%)	RMSE	MAE
100	F4 weekly	78	75	81	0.43	0.25
50	F4 weekly	83	74	90	0.41	0.28
100	F4 daily	79	70	86	0.41	0.29
100	All weekly	80	68	91	0.37	0.28

3.2. Discussion

This section discusses the datasets used to train the daily and weekly prediction models and the training experiments conducted.

The data set of 10 rain detection parameters in Fig. 3 has a unique distribution. As in parameters 1, 4, and 10, which have distributions only on the positive axis, parameters 3, 6, and 13 are gathered on the negative

axis, parameter 5 has an even distribution on negative and growth, and parameters 8 and 9 which have too much gap between max and min values. If we look at the data distribution of parameter 8, as shown in Fig. 5, and parameter 9, as shown in Fig. 6. Although the gap is significant, both have a dominant frequency between the value 0, as shown in Fig. 7.

Therefore, too large gap values can be considered as noise. The clustering results with the EM-GMM algorithm have a silhouette score 0.5 when n clusters are equal to 3, as shown in Fig. 8. The combination of parameters 8 and 9 has a more significant silhouette score than the combination of several existing parameters. Parameters 8 and 9 have more recommendations for further prediction of more rain or heavy rain.

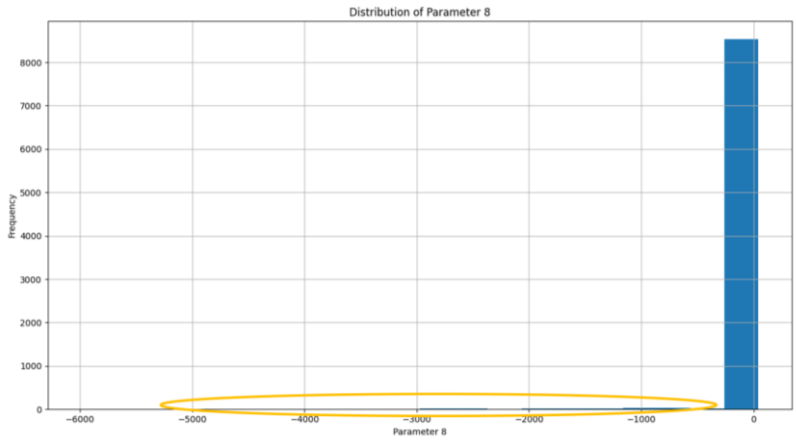

Fig. 5. Data distribution parameters 8

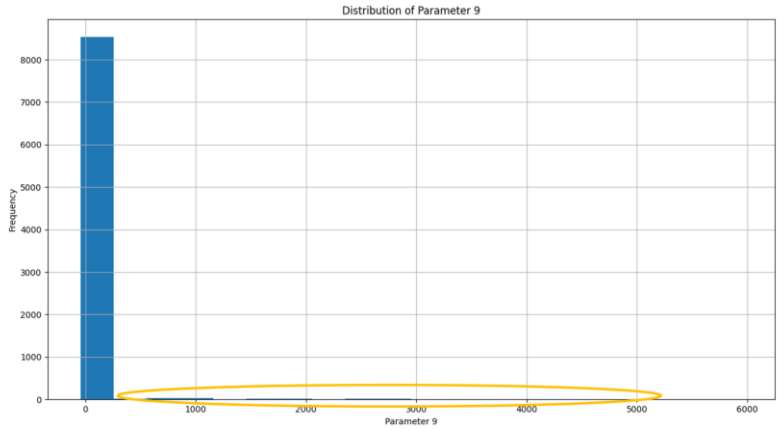

Fig. 6. Data distribution parameters 9

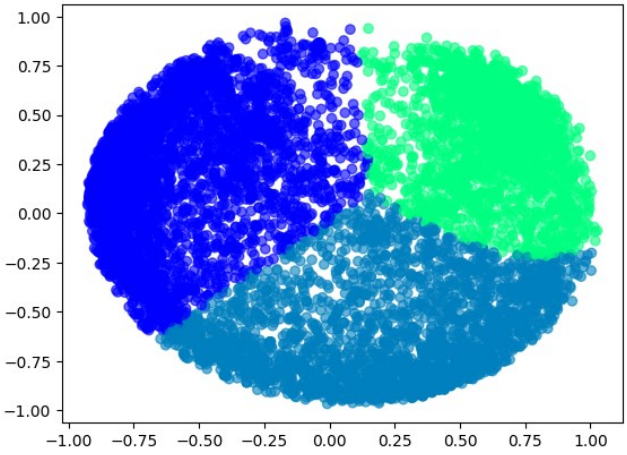

Fig. 7. Domain frequency

Fig. 8. Silhouette score

4. CONCLUSION

This research compares the prediction model using 10 rain detection parameters with daily and weekly LSTM prediction models to detect heavy rain. The training and testing results show that the weekly prediction model has a better accuracy rate, 85%, compared to the daily prediction model, which only reaches 80%. However, when viewed based on the heavy rain label, the daily prediction model provides the highest accuracy of 86%. In addition, further analysis was carried out to compare the distribution of 10 rain detection parameters used as datasets. Using the Expectation-Maximization Gaussian Mixture Model (EM-GMM) algorithm, a silhouette score value 0.5 was obtained when the number of clusters (n) was 3, especially in the combination of the 8th and 9th parameters. Although the 8th and 9th parameters showed poor data distribution, these results open up more opportunities to utilize these parameters as additional datasets in the development of heavy rain prediction models in the future.

REFERENCES

[1] Dwikorita, "BMKG Akui Prediksi Cuaca Tak 100 Persen Akurat" Berita Sains, CNN Indonesia, 22 Januari 2020. [Online]. Available: https://www.cnnindonesia.com/teknologi/20200121141153-199-467306/bmkg-akui-prediksi-cuaca-tak-100-persen-akurat.

[2] J. Byun, C. Jun, J. Kim, J. Cha and R. Narimani, "Deep Learning-Based Rainfall Prediction Using Cloud Image Analysis," in *IEEE Transactions on Geoscience and Remote Sensing*, vol. 61, pp. 1-11, no. 4701411, 2023, https://doi.org/10.1109/TGRS.2023.3263872 .

[3] M. F. Putranto and R. Munir, "Deep Learning Approach for Heavy Rainfall Prediction Using Himawari-8 And RDCA Data," *International Conference on Computer, Control, Informatics and its Applications (IC3INA)*, pp. 424-429, 2023, https:/doi.org/10.1109/IC3INA60834.2023.10285744.

[4] M. M. Hassan *et al*., "Machine Learning-Based Rainfall Prediction: Unveiling Insights and Forecasting for Improved Preparedness," in *IEEE Access*, vol. 11, pp. 132196-132222, 2023, https://doi.org/10.1109/ACCESS.2023.3333876.

[5] N. Srinu and B. H. Bindu, "A Review on Machine Learning and Deep Learning based Rainfall Prediction Methods," *International Conference on Power, Energy, Control and Transmission Systems (ICPECTS)*, pp. 1-4, 2022, https://doi.org/10.1109/ICPECTS56089.2022.10047554.

[6] S. S. Ravi, R. G. K. Sai and J. R. R. R, "Design of Deep Learning Model for Predicting Rainfall," *8th International Conference on Advanced Computing and Communication Systems (ICACCS)*, pp. 1343-1347, 2022, https://doi.org/10.1109/ICACCS54159.2022.9785028.

[7] V. K. Verma, H. S. Janagama and N. Patil, "An Efficient Rainfall Prediction Model Using Deep Learning Method," *Third International Conference on Secure Cyber Computing and Communication (ICSCCC)*, pp. 566-572, 2023, https://doi.org/10.1109/ICSCCC58608.2023.10176598.

[8] Z. He, "Rain Prediction In Australia With Active Learning Algorithm," *International Conference on Computers and Automation (CompAuto)*, pp. 14-18, 2021, https://doi.org/10.1109/CompAuto54408.2021.00010.

[9] Y. Gao and Y. Li, "Prediction of rainfall-type debris flow in Jiangjiagou based on LSTM-Attention," *3rd International Conference on Computer Vision, Image and Deep Learning & International Conference on Computer Engineering and Applications (CVIDL & ICCEA,* pp. 1-6, 2022, https://doi.org/10.1109/CVIDLICCEA56201.2022.9824223.

[10] V. Monita," Rainfall Prediction from Himawari-8 Data Using the Deep Learning Method," *Journal of Wireless Mobile Networks, Ubiquitous Computing, and Dependable Applications (JoWUA)*, vol. 15, no. 2, pp. 47-59, 2024, https://doi.org/10.58346/JOWUA.2024.I2.004.

[11] R. Phadke, G. Mohamad Ramadan, R. Archana Reddy, A. Kumar Pani and H. M. Al-Jawahry, "Prediction of Rainfall Using Seasonal Auto Regressive Integrated Moving Average and Transductive Long Short-Term Model," *International Conference on Ambient Intelligence, Knowledge Informatics and Industrial Electronics (AIKIIE)*, pp. 1-5, 2023, https://doi.org/10.1109/AIKIIE60097.2023.10390346.
[12] K. G, Y. Sushmitha, K. L. Saranya, P. Naga Ramya Sri and P. Amulya, "Rainfall Prediction Using Deep Learning and Machine Learning Techniques," *International Conference on Advances in Computing, Communication and Applied Informatics (ACCAI)*, pp. 1-7, 2023, https:/doi.org/10.1109/ACCAI58221.2023.10199905.
[13] K. Bessho *et al*., "An introduction to Himawari-8/9 — Japan's new-generation geostationary meteorological satellites," *J. Meteorol. Soc. Japan. Ser. II*, vol. 94, no. 2, pp. 151–183, 2016, https://doi.org/10.2151/jmsj.2016-009.
[14] F. Zhang, X. Wang, J. Guan, M. Wu, and L. Guo, "Rn-net: A deep learning approach to 0–2 h rainfall nowcasting based on radar and automatic weather station data," *Sensors,* vol. 21, no. 6, pp. 1–14, 2021, https://doi.org/10.3390/s21061981.
[15] S. Kawasaki, Q. Wang, "Insolation Forecasting by using Image-processed Satellite Images Data and Forecasting of Cloud Imageries," *IEEJ Transactions on Power and Energy*. vol.142, pp. 525-532, 2022, https://doi.org/10.1541/ieejpes.142.525.
[16] R. Lagerquist, J. Q. Stewart, I. Ebert-Uphoff, C. Kumler, "Using deep learning to nowcast the spatial coverage of convection from Himawari-8 satellite data," *Monthly Weather Review*, vol 149, no. 12, pp. 3897–3921, 2021, https://doi.org/10.1175/mwr-d-21-0096.1.
[17] Y. Sawada, K. Okamoto, M. Kunii, T. Miyoshi, "Assimilating every- 10-minute Himawari-8 infrared radiances to improve convective predictability," *Journal of Geophysical Research: Atmospheres*, vol.124, pp. 2546–2561, 2019, https://doi.org/10.1029/2018JD029643.
[18] T. T. K, Tran, S. M. Bateni, S. J. Ki, H. Vosoughifar, "A Review of Neural Networks for Air Temperature Forecasting. *Water (Swiss)*, vol. 13, no. 9, pp. 1–15, 2021, https://doi.org/10.3390/w13091294.
[19] W. Liu *et* al., "Fall Detection for Shipboard Seafarers Based on Optimized BlazePose and LSTM," *Sensor*, vol. 22, p. 5449, 2022, https://doi.org/doi.org/10.3390/s22145449.
[20] L. Song, G. Yu, J. Yuan, Z. Liu, "Human pose estimation and its application to action recognition: A survey," *Journal of Visual Communication and Image Representation*, vol 76, 103055, 2021, https://doi.org/10.1016/j.jvcir.2021.103055.
[21] T. Tashima, T. Kubota, T. Mega, T. Ushio and R. Oki, "Precipitation Extremes Monitoring Using the Near-Real-Time GSMaP Product," *in IEEE Journal of Selected Topics in Applied Earth Observations and Remote Sensing*, vol. 13, pp. 5640-5651, 2020, https://doi.org/10.1109/JSTARS.2020.3014881.
[22] M. Momin, M. M. Alam, M. M. Hasan Mahfuz, M. R. Islam, M. Hadi Habaebi and K. Badron, "Prediction of Rain Attenuation on Earth-to-satellite Link using Rain Rate Measurement with Various Integration Times," *8th International Conference on Computer and Communication Engineering (ICCCE),* pp. 385-390, 2021, https://doi.org/10.1109/ICCCE50029.2021.9467173.
[23] S. Ramanjaneyulu, S. E. Khaleelullla, R. K. Tenali, A. Rudraraju, S. Kaliappan and S. K. Pathuri, "Enhanced Rainfall Prediction: Leveraging Ensembling Models for Maximum Forecasting Performance," *3rd International Conference for Advancement in Technology (ICONAT)*, pp. 1-7, 2024, https://doi.org/10.1109/ICONAT61936.2024.10774805.
[24] G. Luo, L. Wang, Y. Zeng, Z. Chen, S. Wen and M. Zhang, "ESM-LSTM based optimisation model for weather prediction," *5th International Conference on Big Data & Artificial Intelligence & Software Engineering (ICBASE)*, pp. 79-83, 2024, https://doi.org/10.1109/ICBASE63199.2024.10762687.
[25] K. Gupta, R. K. Gupta and A. Gupta, "Daily, Weekly and Monthly Rain Forecasting using Deep Learning," *3rd International Conference for Innovation in Technology (INOCON)*, pp. 1-6, 2024, https://doi.org/10.1109/INOCON60754.2024.10511700.
[26] S. Gupta, A. Moledina, S. Athavale, S. Gajare and M. Kate, "Air Quality Prediction Using Machine Learning: A Comparative Study," *6th International Conference on Advances in Science and Technology (ICAST)*, pp. 485-489, 2023, https://doi.org/10.1109/ICAST59062.2023.10454930.
[27] Maimunah, J. L. Buliali and A. Saikhu, "The Use of LSTM Model with Lagged Daily Inputs for Waste Disposal Prediction," *Eighth International Conference on Informatics and Computing (ICIC)*, pp. 1-6, 2023, https://doi.org/10.1109/ICIC60109.2023.10382040.
[28] H. Rumapea, M. Sinambela, I. K. Jaya and I. M. Sarkis, "Prediction of Rainfall in North Sumatera Using Machine Learning," *International Conference of Computer Science and Information Technology (ICOSNIKOM)*, pp. 1-4, 2023, https://doi.org/10.1109/ICoSNIKOM60230.2023.10364504.
[29] S. K. Gupta, P. Bhardwaj, R. Kumar, Pragya and A. Bag, "Rain-Prediction-system-Incorporated Automatic Water Feeding System for Agriculture Application," *9th International Conference on Smart Computing and Communications (ICSCC)*, pp. 173-177, 2023, https://doi.org/10.1109/ICSCC59169.2023.10335025.
[30] P. Paul, S. Basak and A. Khan, "A rainfall prediction system using Machine Learning (ML) and Internet of Things (IoT)," *8th International Conference on Computing in Engineering and Technology (ICCET 2023), Hybrid Conference*, pp. 393-398, 2023, https://doi.org/10.1049/icp.2023.1522.
[31] R. Kumar and S. Arnon, "Experimental Modeling of Short-Term Effects of Rain on Satellite Link Using Machine Learning," *in IEEE Transactions on Instrumentation and Measurement*, vol. 72, no. 5503812, pp. 1-12, 2023, https://doi.org/10.1109/TIM.2023.3306825.
[32] P. P. G. Jaiswal *et al*., "A Stacking Ensemble Learning Model for Rainfall Prediction based on Indian Climate," *6th International Conference on Information Systems and Computer Networks (ISCON)*, pp. 1-6, 2023,https://doi.org/10.1109/ISCON57294.2023.10112077.

[33] C. Vijayalakshmi, K. Sangeeth, R. Josphineleela, R. Shalini, K. Sangeetha and D. Jenifer, "Rainfall Prediction using ARIMA and Linear Regression," *International Conference on Computer, Power and Communications (ICCPC),* pp. 366-370, 2022, https://doi.org/10.1109/ICCPC55978.2022.10072125.
[34] N. Srinu, S. Sivahari and M. R. Kale, "Leveraging Radial Basis Function Neural Networks for Rainfall Prediction in Andhra Pradesh," *International Conference on Computer, Power and Communications (ICCPC)*, pp. 474-477, 2022, https://doi.org/10.1109/ICCPC55978.2022.10072177.
[35] L. Quibus, V. Le Mire, J. Queyrel, L. Castanet and L. Féral, "Rain Attenuation Estimation with the Numerical Weather Prediction Model WRF: Impact of Rain Drop Size Distribution for a Temperate Climate," *15th European Conference on Antennas and Propagation (EuCAP)*, pp. 1-5, 2021, https://doi.org/10.23919/EuCAP51087.2021.9410927.
[36] T. Tashima, T. Kubota, T. Mega, T. Ushio and R. Oki, "Precipitation Extremes Monitoring Using the Near-Real-Time GSMaP Product," *in IEEE Journal of Selected Topics in Applied Earth Observations and Remote Sensing*, vol. 13, pp. 5640-5651, 2020, https://doi.org/10.1109/JSTARS.2020.3014881.
[37] X. Zhou, "Stock Price Prediction using Combined LSTM-CNN Model," *3rd International Conference on Machine Learning, Big Data and Business Intelligence (MLBDBI)*, pp. 67-71, 2021, https://doi.org/10.1109/MLBDBI54094.2021.00020.
[38] S. Zhu, J. Yao and S. Z. Djokic, "Comparison of Two Modified Deterministic LSTM Models with a Probabilistic LSTM Model for a Day-Ahead Forecasting of Electricity Demands," *IEEE Belgrade PowerTech*, pp. 1-6, 2023, https://doi.org/10.1109/PowerTech55446.2023.10202847.
[39] Y. K. Joshi, U. Chawla and S. Shukla, "Rainfall Prediction Using Data Visualisation Techniques," *10th International Conference on Cloud Computing, Data Science & Engineering (Confluence),* pp. 327-331, 2020, https://doi.org/10.1109/Confluence47617.2020.9057928.
[40] B. Setya, R. A. Nurhidayatullah, M. B. Hewen and K. Kusrini, "Comparative Analysis Of Rainfall Value Prediction In Semarang Using Linear And K-Nearest Neighbor Algorithms," *5th International Conference on Cybernetics and Intelligent System (ICORIS)*, pp. 1-5, 2023, https://doi.org/10.1109/ICORIS60118.2023.10352274.
[41] N. Tiwari and A. Singh, "A Novel Study of Rainfall in the Indian States and Predictive Analysis using Machine Learning Algorithms," *International Conference on Computational Performance Evaluation (ComPE)*, pp. 199-204, 2020, https://doi.org/10.1109/ComPE49325.2020.9200091.
[42] P. V. S. Krithik, M. T. A. Raghavan, S. P. K and K. Vasanth, "Real Time Rainfall Prediction for Hyderabad Region using Machine learning Approach," *Innovations in Power and Advanced Computing Technologies (i-PACT)*, pp. 1-6, 2021, https://doi.org/10.1109/i-PACT52855.2021.9697017.
[43] A. Raut, D. Theng and S. Khandelwal, "Random Forest Regressor Model for Rainfall Prediction," *International Conference on New Frontiers in Communication, Automation, Management and Security (ICCAMS)*, pp. 1-6, 2023, https://doi.org/10.1109/ICCAMS60113.2023.10526085.
[44] C. Z. Basha, N. Bhavana, P. Bhavya and S. V, "Rainfall Prediction using Machine Learning & Deep Learning Techniques," *International Conference on Electronics and Sustainable Communication Systems (ICESC)*, pp. 92-97, 2020, https://doi.org/10.1109/ICESC48915.2020.9155896.

BIOGRAPHY OF AUTHORS

Vivi Monita, graduated from the School of Electrical Engineering (Telecommunications), Telkom University, Bandung, Indonesia, in 2021 and 2023 with her Bachelor's degree (S.T.) and Master's Degree (M.T.). She is currently a full-time lecturer at Telkom University Jakarta Campus. Email: monitavivii@telkomuniversity.ac.id

Sevierda Raniprima, graduated from the School of Electrical Engineering (Telecommunications), Telkom University, Bandung, Indonesia, in 2014 with a Bachelor's degree (S.T.) and 2016 and a Master's Degree (M.T.) in Institut Teknologi Bandung (ITB). She is currently a full-time lecturer at Telkom University Jakarta Campus. Email: sevierdar@telkomuniversity.ac.id

Nanang Cahyadi, graduated from the Institut Teknologi Nasional Bandung (ITENAS) in 2018 with a Bachelor's degree (S.T.) and in 2021 a Master's Degree (M.T.) in Institut Teknologi Bandung (ITB). He is currently a full-time lecturer at Telkom University Jakarta Campus. Email: nanangcahyadi@telkomuniversity.ac.id